King Saud University

Arabian Journal of Chemistry

www.ksu.edu.sa
www.sciencedirect.com

ORIGINAL ARTICLE

Ultrasonic green synthesis of silver nanoparticles mediated by Pectin: Characterization and evaluation of the cytotoxicity, antioxidant, and colorectal carcinoma properties

Dongxiao Wang [a,1], **Wei Geng** [b,1], **Qingxia Li** [c], **Guoxian Li** [a], **Donglin Zhang** [a], **Haiqing Zhang** [d,*]

[a] *Department of Emergency, Meizhou People's Hospital, Meizhou, GuangDong 514000, China*
[b] *VIP Health Management Center, Xi'an International Medical Center Hospital, Xi'an, Shaanxi 710100, China*
[c] *Department of Obstetrics and Gynecology, Meizhou Hospital of TCM, Meizhou, GuangDong 514071, China*
[d] *Department of Colorectal Surgery, Shanghai Jiao Tong University Affiliated Sixth People's Hospital South Campus, Shanghai 201499, China*

Abstract Regarding applicative, facile, green chemical research, a bio-inspired approach is being reported for the synthesis of Ag nanoparticles by pectin as a natural reducing and stabilizing agent without using any toxic and harmful reagent. The biosynthesized Pectin/Ag NPs were characterized by advanced physicochemical techniques like ultraviolet–visible (UV–Vis), Fourier Transformed Infrared spectroscopy (FT-IR), Scanning Electron Microscopy (SEM), High-Resolution Transmission Electron Microscopy (HR-TEM), Energy Dispersive X-ray spectroscopy (EDX), and X-ray Diffraction (XRD) study. It has been established that pectin-stabilized silver nanoparticles have a spherical shape with a mean diameter from 15 to 20 nm. After that, the biological performance of those biomolecules functionalized Ag NPs was investigated. In the MTT assay, human colorectal carcinoma (HCT-8 [HRT-18], Ramos.2G6.4C10, HT-29, and HCT 116) and normal cell lines (HUVEC) were used to study the cytotoxicity and anticancer potential of human colorectal over the $AgNO_3$ and Pectin/Ag NPs. The cell viability of Pectin/Ag NPs was very low against human colorectal carcinoma cell lines without any cytotoxicity on the normal (HUVEC) cell line. The best anti-human colorectal carcinoma properties of Pectin/Ag NPs against the above cell lines was in the

---

* Corresponding author.
E-mail address: haiqingzhang1981@sina.com (H. Zhang).
[1] Dongxiao Wang and Wei Geng are co-first authors, they contributed equally to this work.

case of the HCT 116 cell line. The antioxidant properties of the AgNO$_3$ and Pectin/Ag NPs were calculated against DPPH free radicals. The IC50 of Pectin/Ag NPs was 167 μg/mL. According to the above results, the Pectin/Ag NPs may be administrated to treat human colorectal carcinoma in humans.

1. Introduction

Colon cancer or colorectal cancer is one of the most important cancers in the gastrointestinal system. Exercise most days of the week, eat a variety of whole grains, fruits, and vegetables, stop smoking, and maintain a healthy weight reduce the occurrence of the colon cancer (Juul et al., 2018; Astin et al., 2011; Cunningham et al., 2010; Lauby-Secretan et al., 2016). The polyps personal history, obesity, smoking, inflammatory intestinal conditions, inherited syndromes, radiation therapy, diabetes, colon cancer family history, older age, high-fat diet, alcohol, African-American race, and sedentary lifestyle are the main risk factors of the colon cancer (Juul et al., 2018; Astin et al., 2011). The colon cancer signs are weight loss, blood in the stool, nausea or vomiting, worsening constipation, anemia or rectal bleeding, change in bowel movements, loss of appetite, decrease in stool caliber, and feeling tired all the time (Juul et al., 2018; Astin et al., 2011). Radiation therapy, targeted therapy, immunotherapy, chemotherapy, and surgery are the therapeutically options of the colon carcinoma (Lauby-Secretan et al., 2016). Due to the high side effects of chemotherapy, the researchers are following the new formulations such as metallic nanoparticles to treat the colon carcinoma (Shaib et al., 2013).

Today, nanoparticles have become very popular due to their wide applications in biology and medicine. Structurally, their size is in the range of 100 nm (Shaib et al., 2013; Raut et al., 2010). In general, there are various physical and chemical methods such as chemical reduction, photochemical reduction, ultraviolet and microwave radiation and laser for the synthesis of metallic nanoparticles. Chemical methods do not work well due to the production of toxic chemical compounds and compared to other methods, environmentally friendly bio-methods are preferred for the synthesis of metallic nanoparticles, as these methods are single-step and do not require reducing and stabilizing compounds (Raut et al., 2010). Biological methods are suitable options for the synthesis of metallic nanoparticles so that the rate of metallic ion reduction is very high. Biological methods are low cost and high yield and lead to the production of nanoparticle crystal structures of different sizes and this depends on the nature of the plant extract, pH, temperature and incubation time (Raut et al., 2010; Varma et al., 2012).

A wide range of medial supplements such as small hydrophilic and hydrophobic vaccines, drugs, and molecules of biological nanoparticles may be administered by the metallic nanoparticles (Raut et al., 2010; Varma et al., 2012). They are widely used in improving the treatment and diagnosis of diseases. Nanoparticles in the form of nanofibers, carbon nanotubes, nanoliposomes, nanospheres widely have been administrated for cell scaffolding and drug carriers. (Raut et al., 2010; Varma et al., 2012; Krishnaraj et al., 2010; Rajeshkumar et al., 2012) Applications of nanoparticles in drug delivery include drug carriers in disorders such as tumor, cardiovascular disease, Alzheimer's. The use of these nanocarriers is very effective for neurological diseases such as Alzheimer's because these nanoparticles can cross the blood–brain barrier due to their size that this barrier has always been a barrier to the passage of drugs to the affected area in this type of destructive brain disease (Shaib et al., 2013; Raut et al., 2010; Varma et al., 2012). Due to the metallic nanoparticles low size, they can also be used in several cancers. The main aim in making metallic nanoparticles is to control the surface properties, particle size, and release of a specific and efficient drug in a specific place and time for the drug to be as effective as possible (Raut et al., 2010; Varma

et al., 2012). Nanoparticles have many therapeutic applications and have always been used to treat various diseases. Their use in the cure of infectious, fungal, bacterial, viral, cutaneous, cardiovascular diseases has been amazing (Varma et al., 2012).

The silver nanoparticles have unique properties to treat several cancers (Krishnaraj et al., 2010; Rajeshkumar et al., 2012; Ahmeda et al., 2020). Silver nanoparticles disrupt cellular communication, disrupting cellular communication networks and involved in DNA damage and in increasing the expression of the apoptotic protein molecule and in initiating programmed cell death of apoptosis. Therefore, they lead to the proliferation of death signals, which is very important in treating cancer (Varma et al., 2012; Krishnaraj et al., 2010; Rajeshkumar et al., 2012; Ahmeda et al., 2020). Hemmati et al. (2019) showed that silver nanoparticle-chitosan composite had excellent anti-acute myeloid leukemia against Human HL-60/vcr cell line (Ahmeda et al., 2020).

In this study we have described ultrasonic green synthesis of the stable pectin stabilized silver nanoparticles (Pectin/Ag NPs) with desirable properties (Scheme 1). We assessed the effects of AgNO$_3$ and Pectin/Ag NPs in the cytotoxicity studies against common human colorectal carcinoma cell lines i.e., HCT-8 [HRT-18], Ramos.2G6.4C10, HT-29, and HCT 116, *in-vitro* for the first time. Also, the antioxidant properties of the AgNO$_3$ and Pectin/Ag NPs were calculated against DPPH free radicals.

2. Experimental

2.1. Materials and methods

The chemicals required for catalyst synthesis and catalyst applications were purchased from Sigma Aldrich. Pectin extracted from citrus peel.

2.2. Synthesis of Pectin/Ag NPs

To initiate the reaction, 20 ml of a freshly prepared aqueous solution of AgNO$_3$ (10 mM) was added to 50 ml of an aqueous pectin solution (1%) under ultrasonic conditions (60 Hz) and left for 10 min at 60 °C. Then the pH of the solution was adjusted to 11.0 (NaOH, 3 wt%) and the reaction mixture was kept with sonication at 60 °C for 60 min. The progress of the reaction is monitored by the change in color from watery yellow to brown color (Krishnaraj et al., 2010) and SPR band which both confirmed the synthesis of silver nanoparticles (Rajeshkumar et al., 2012). The prepared Pectin/Ag NPs were collected by centrifugation and washed several times with DI-water.

2.3. Assessment of anti-human colorectal carcinoma potentials of AgNO$_3$ and Pectin/Ag NPs

In this assay, following human colorectal carcinoma and normal cell lines were used to study the cytotoxicity and anti-cancer potential of human colorectal over the AgNO$_3$ and Pectin/Ag NPs using the MTT assay:
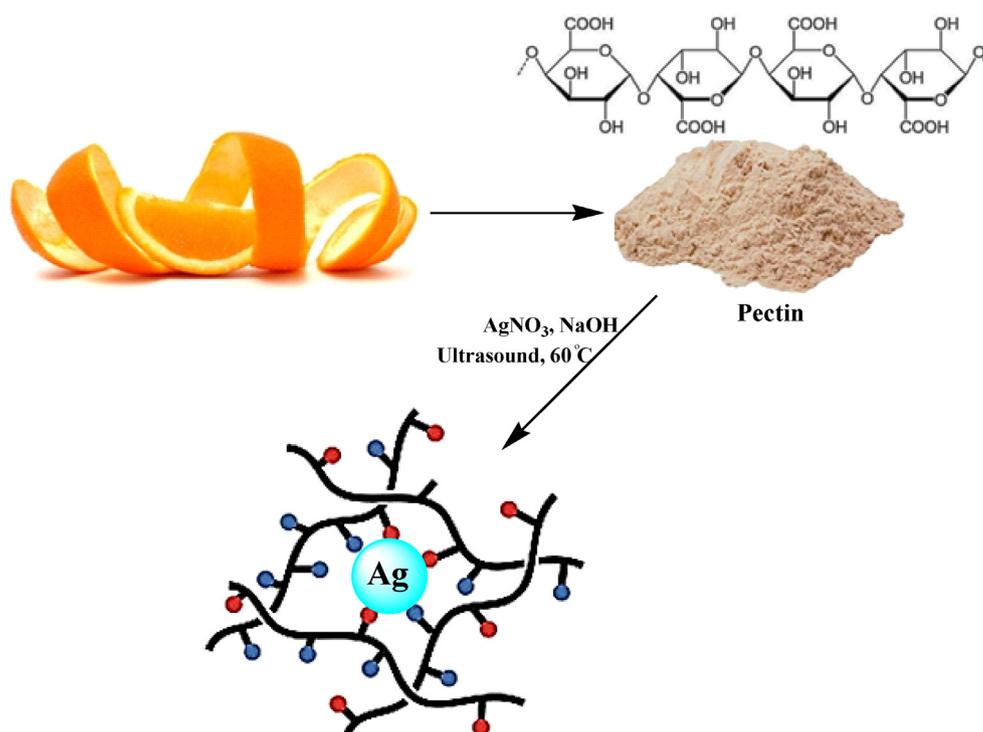
Scheme 1   Preparation of Pectin/Ag NPs under ultrasound conditions.

(1) Human colorectal carcinoma cell lines: Colorectal adenocarcinoma (HT-29), colorectal carcinoma (HCT 116), ileocecal colorectal adenocarcinoma (HCT-8 [HRT-18]), and Burkitt's lymphoma (Ramos.2G6.4C10).
(2) Normal cell line: HUVEC.

15 ml of RPMI 1640 medium containing 10 % FSC (10 mg/ml penicillin and 100 mg/ml streptomycin) in a culture flask, placed in a CO_2 incubator for 2 h to equilibrate the medium. Under safe conditions (using insulated gloves and goggles) the frozen cell vial was removed from the nitrogen storage tank. To avoid the possibility of explosion of the vial (due to the possible entry of liquid nitrogen into the vial), loosen the lid, after disinfecting the outer surface of the vial with 70 % alcohol, under the hood to remove nitrogen gas. Close the vial lid again and immediately melt it in a pan at 37 °C. The melting process should be completed in about 1 min and the cells should be avoided from overheating. The medium was added dropwise to the vial and then its contents were taken out and centrifuged with the medium in 15 ml sterile test tubes. After centrifugation, the supernatant was removed and the cells were suspended again in the medium and transferred to a pre-prepared flask containing the medium and FBS and incubated (Ahmeda et al., 2020).

Cell line used in RPMI 1640 medium containing penicillin (100 IU/ml), streptomycin (100 IU/ml), glutamine (2 mmol) and 10 % fetal bovine serum (FBS). They were incubated at 37 °C and in an atmosphere containing 0.5 CO_2. Cells began to grow in 75 cm^2 T-flasks in 15 ml medium with an initial number of $1–2 \times 10^6$ cells. After three days and covering the flask bed with the cell, the adhesive layer to the bottom of the flask was separated enzymatically using trypsin-verson and transferred to a sterile test tube for 10 min at 1200 rpm.

The cells were then suspended in a fresh culture medium with the help of a Pasteur pipette and the suspension was poured into 100-well plate flat wells (for cell culture) using an 8-channel sampler of 100 µl. One column of wells was kept cell-free and as a plank containing only culture medium. In another column, it was considered to contain culture medium and healthy cells and in other columns, it was considered to contain culture medium and cell line cells. One of these columns, which contained culture medium and cells and did not contain $AgNO_3$ and Pectin/Ag NPs was considered as a control (Ahmeda et al., 2020).

The plates were incubated in the incubator for 24 h to return the cells to normal from the stress of trypsinization. After this time, suitable dilutions of the prepared $AgNO_3$ and Pectin/Ag NPs (0–1000 µl/ml) and 100 µl of each dilution were added columnar to the plate wells (Thus, the final concentration of the studied compound in the wells was halved. Therefore, the concentrations were prepared twice as much to reach the final concentration after being added to the well). The cells were incubated for 37 h at 37 °C and 5% CO_2 in the atmosphere. After 72 h, 20 µl of MTT solution (5 mg/ml) was added to each well. The plates were incubated for 3 to 4 h and then the residue was removed and 100 µl of DMSO was added to each well to dissolve the resulting formazan. After 10 min, using shaking the plates, the optical absorption of Formazan at 570 nm was read using a plate reader. Wells containing cells without $AgNO_3$ and Pectin/Ag NPs were considered as control and the optical density of wells without cells and only culture medium were considered as blank. The percentage of cell viability was calculated using the following formula (Ahmeda et al., 2020):

$$Cell\ viability(\%) = \frac{Sample\ A}{Control\ A} \times 100$$

The closer is the obtained value to the IC50 of AgNO$_3$ and Pectin/Ag NPs, the stronger is the cell viability activity of the material. The graph of the IC50 of the AgNO$_3$ and Pectin/Ag NPs was produced by drawing the percent inhibition curve versus the AgNO$_3$ and Pectin/Ag NPs concentration. First, three stock samples with variable concentrations (0–1000 μg/ml) of AgNO$_3$ and Pectin/Ag NPs were prepared. Then, a serial dilution was prepared from each sample, and IC50 of the above samples was measured separately, following which their mean was calculated (Ahmeda et al., 2020).

2.4. Evaluation of the antioxidant property of AgNO$_3$ and Pectin/Ag NPs

Analysis of antioxidant capacity by DPPH radical method is a well-known test for measuring the antioxidant power of various compounds. The basis of this method is based on the reduction of free radical DPPH by antioxidants in the absence of other free radicals in the environment. A compound is generally compared to a known antioxidant compound such as Butylated Hydroxytoluene (BHT). Analysis of antioxidant capacity by DPPH method is a test that has received much attention in the fields of food, pharmaceuticals and biotechnology and is used to develop and introduce new antioxidants. The basis of this method is based on the reduction of free radical DPPH by antioxidants in the absence of other free radicals in the environment, which results in color in the environment whose intensity can be measured by spectroscopy. DPPH is a stable free radical that has an unpaired electron on one of the nitrogen bridge atoms. Radical inhibition of DPPH is the basis for assessing antioxidant capacity (Ahmeda et al., 2020):

$$DPPH^{\circ}\ (purple) + H - A \rightarrow\ DPPHH\ (yellow)\ +\ A^{\circ}$$

DPPH is a stable radical whose methanolic solution has a purple color that shows the highest light absorption at 519–595 nm. The basis of this method is that the DPPH radical acts as an electron acceptor of a donor molecule such as an antioxidant, thus converting DPPH to DPPH$_2$. In this case, the purple color of the environment turns yellow, so the absorption intensity decreases to 595 nm. Antioxidant properties can be determined by measuring the decrease in adsorption intensity by spectroscopy (Ahmeda et al., 2020).

In the present study to measure the antioxidant properties of AgNO$_3$ and Pectin/Ag NPs, 2 ml of DPPH (100 μM) dissolved in methanol with 2 ml of AgNO$_3$ and Pectin/Ag NPs at the concentrations of μg/ml. The resulting mixture was placed at 25 °C for 30 min. Then the samples absorbance was measured at 520 nm by spectrophotometer (Spectramax Gemini XS; Molecular Devices, Sunnyvale, CA) and the amount of antioxidant effect was determined by the below formula (Ahmeda et al., 2020):

$$\%Inhibition = \left[(A_{blank} - A_{sample}) / A_{blank} \right] \times 100$$

The blank sample consisted of a mixture of 2 ml of AgNO$_3$ and Pectin/Ag NPs and 2 ml of methanol and a sample containing 2 ml of DPPH and 2 ml of AgNO$_3$ and Pectin/Ag NPs with the concentrations used was considered as negative control. BHT was also used as a positive control. Calculating the 50 % inhibition error (IC50) is an excellent way to compare drug activity that dose in which 50% of the final activity of the drug occurs is the criterion for measurement and comparison.

In this test, the amount of IC50 for different repetitions of the test was also calculated and is compared with IC50 of BHT molecule, which is an indicator of antioxidant activity. The closer IC50 is to BHT, the stronger the antioxidant activity. In the following experiments, the inhibition concentration of 50 % of AgNO$_3$ and Pectin/Ag NPs was calculated by plotting the inhibition percentage curve against the AgNO$_3$ and Pectin/Ag NPs concentration. In the next step, a serial dilution was prepared from each sample and 50 % inhibition concentration of three separate samples was measured and its mean was calculated. All experiments were performed three times (Ahmeda et al., 2020).

2.5. Qualitative measurement

The obtained results were loaded into the "SPSS-22" program and evaluated by "one-way ANOVA", accompanied by a "Duncan post-hoc" check ($P \leq 0.01$).

3. Results and discussion

3.1. Structural characterization of Pectin/Ag NPs

Silver nanoparticles capped by pectin macromolecules were fabricated by a 'green' awapproach via chemical reduction of Ag$^+$ cations under ultrasonic condition (Scheme 1). The polysaccharide pectin is acted as a reducing and stabilizing agent in this work. V. Kulikouskaya et al. (Al-Muhanna et al., 2015; Hileuskaya et al., 2020), and P. Pallavicini et al. (Pallavicini et al., 2017), shown earlier the fabrication of silver nanoparticles by the pectin. Free hemiacetal hydroxy groups in the pectin macromolecule determine its reducing properties in an alkaline medium. The arabinans and galactans from the pectin also contain hydroxyl groups capable of exhibiting the reducing properties.

The synthesized Pectin/Ag NPs were analyzed using UV–Vis, FT-IR spectroscopy, FE-SEM, EDX TEM, and XRD techniques. The successful biogenic synthesis of Ag NPs was primarily confirmed by a visual color change from yellow to dark red. The synthesis of Ag NPs was next justified by UV–Vis spectroscopy. Fig. 1 shown the band of Ag NPs, being observed at around 430 nm (λ_{max}). The appearance band at a wavelength of about 430 nm after the green synthesis process, was evidence that the Ag^{1+} cation became completely reduced by time.

Fig. 2 displays the FT-IR spectra of Pectin/Ag NPs. The broad peak that appeared at 3425 cm^{-1} corresponds to the overlapped stretching vibrations of OH groups (Ahmeda et al., 2020). The alcoholic C–O stretching and O–H bending peaks are observed at 1065 cm^{-1} and 1620 cm^{-1}, respectively Ahmeda et al., 2020). This is attributed to the strong complexation of Ag NPs with the pectin and OH functions.

The surface morphology of the Pectin/Ag NPs was investigated by the FE-SEM study, as shown in Fig. 3. It shown the quasi-spherical shaped nanoparticles of mean diameter ∼ 15–20 nm. For further structural inherence of the nanocomposite, HR-TEM analysis was carried out (Fig. 4). The HR-TEM measurements revealed the presence of spherically shaped nanoparticles in the matrix (Fig. 4). The mean diameter of Ag NPs was in the range of ∼ 15–20 nm. In the image, the nanoparticles were well dispersed without any aggregation.
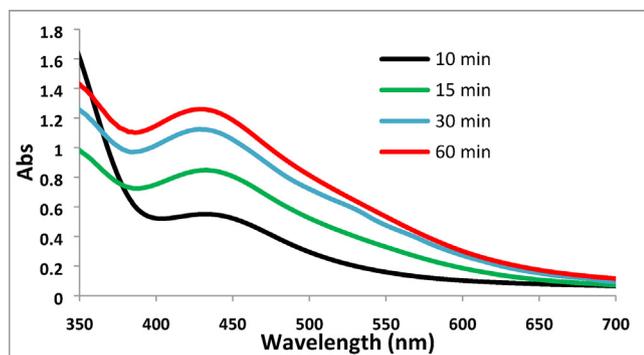
Fig. 1 UV–visible absorption spectra of Pectin/Ag NPs.

Moreover, Fig. 5 determines the particle size distribution histogram for Pectin/Ag NPs whose average size are approximately 17.67 nm.

The elemental composition of Pectin/Ag NPs was determined by EDX analysis. As depicted in Fig. 6, the profile displays and confirms the presence of Ag in the composite. Again, the signals corresponding to C and O atoms can be ascribed to pectin molecules thereby assuring the proposed nanostructure.

The crystalline nature of the obtained Ag nanoparticles was further determined by XRD analysis. The typical XRD pattern of Pectin/Ag NPs is exhibited in Fig. 7, illustrating the crystalline nature of synthesized Ag NPs. From the XRD pattern, four distinct diffraction peaks at 38.3°, 44.3°, 64.7° and 77.4° are indexed as (111), (200), (220) and (311) planes of *fcc* metallic silver.
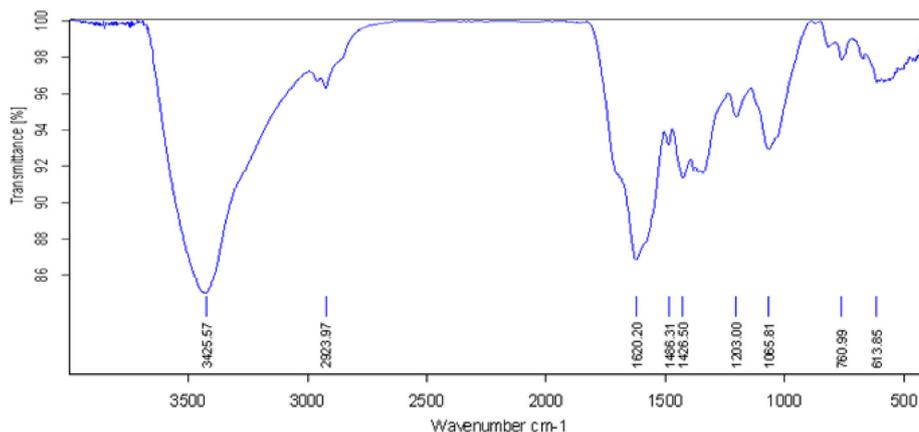
Fig. 2 FT-IR analysis of Pectin/Ag NPs.
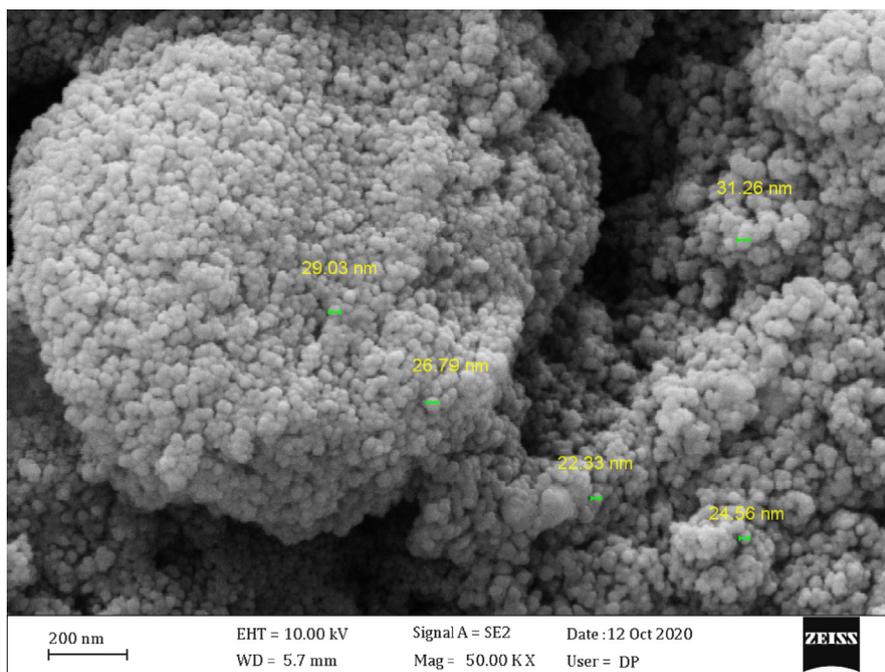
Fig. 3 FE-SEM image of the Pectin/Ag NPs.

Fig. 5 The particle size distribution histograms for Pectin/Ag NPs.

Fig. 4 HR-TEM images of Pectin/Ag NPs.

Furthermore, the stability of Ag NPs was monitored TEM image by UV–Vis spectroscopy (Fig. 8) after 60 days, the synthesized silver nanoparticles by this method are relatively stable with no significant variance in the shape, position and symmetry of the absorption peak even after two months.

3.2. Anti-human colorectal carcinoma potentials of AgNO₃ and Pectin/Ag NPs

The MTT assay is a procedure of colorimetric based on reducing and breaking of yellow tetrazolium crystals by the enzyme succinate dehydrogenase to form insoluble purple crystals. In this method, unlike other methods, the steps of washing and collecting cells, which often cause the loss of a number of cells and increase the work error, have been eliminated and all test steps from the beginning of cell culture to reading the results with a photometer are performed on a microplate, so the repeatability, accuracy and sensitivity of the test are high

(Ahmeda et al., 2020). If the test is performed on cells attached to the plate, an appropriate number of cells (about 2,000 cells) must first be cultured in each of the wells. Then we select the control and test wells and add the appropriate amount of mitogen or drug to the test wells and place the plate in the incubator for the required time so that the desired substance affects the cells (Shaib et al., 2013; Raut et al., 2010). At the end of the incubation time, discard the supernatant and add 200 μl of culture medium containing half an mg/ml of MTT solution to each well and put it again in a carbon dioxide incubator for 2 to 4 h at 37 °C. During incubation, MTT is regenerated by one of the enzymes of the mitochondrial respiratory cycle i.e., succinate dehydrogenase. The regeneration and breakage of this ring produce purple-blue crystals of formazan that are easily detectable under a microscope. At the end, the optical absorption of the resulting solution can be read at 570 nm and the cells number can be calculated using a standard curve. For each cell line, there is a linear relationship between the number of cells and the light absorption of the final solution. Therefore, to examine each cell type, a standard curve related to the same cell line must be drawn and used (Varma et al., 2012; Krishnaraj et al., 2010; Rajeshkumar et al., 2012; Ahmeda et al., 2020).

In the present study, the cytotoxicity of AgNO₃ and Pectin/Ag NPs was explored by studying its interaction with normal (HUVEC) and human colorectal carcinoma cell lines i.e. colorectal adenocarcinoma (HT-29), colorectal carcinoma (HCT 116), ileocecal colorectal adenocarcinoma (HCT-8 [HRT-18]), and Burkitt's lymphoma (Ramos.2G6.4C10) by MTT assay for 48 h. The interactions being expressed as cell viability (%) were observed at different AgNO₃ and Pectin/Ag NPs concentrations (0–1000 μg/mL) with the five cell lines which have been shown in details in Figs. 9 and 10. In all the cases, the % cell viability gets reduced with increasing AgNO₃ and Pectin/Ag NPs sample concentrations.

The IC50 of Pectin/Ag NPs against Ramos.2G6.4C10, HCT-8 [HRT-18], HCT 116, and HT-29 were 485, 393, 236, and 262 μg/mL, respectively. Thereby, the best cytotoxicity results and anti-human colorectal carcinoma potentials of our Pectin/Ag NPs was observed in the case of the HCT 116 cell line (Table 1) (see Table 2).

Among the different parameters of metallic nanocomposites such as, size, texture and nature of surface functions, the size effect is most essential in the anticancer assay using
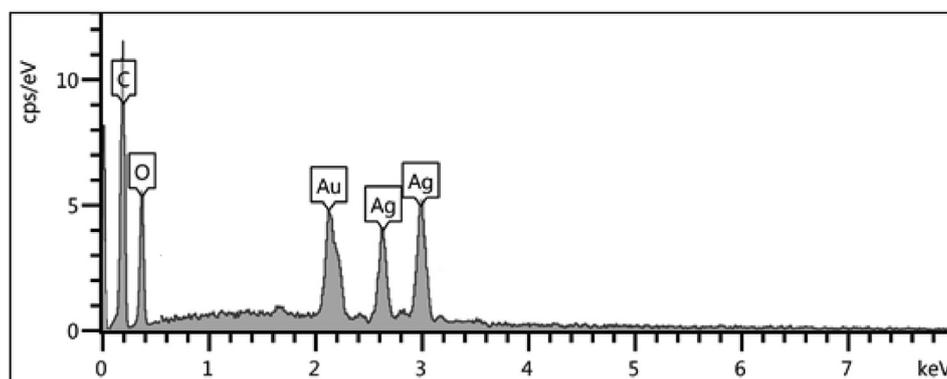
Fig. 6 EDX spectrum of the Pectin/Ag NPs.
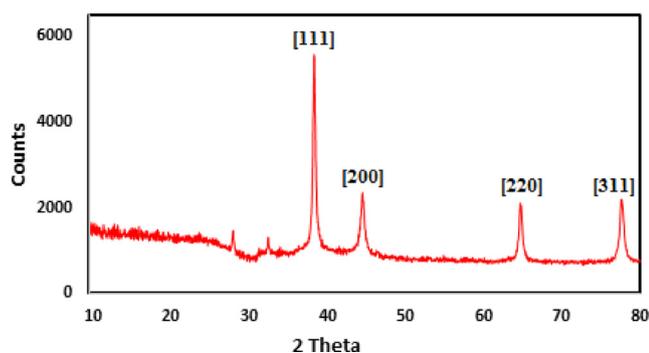
Fig. 7 X-ray diffraction analysis of synthesized Pectin/Ag NPs.

standard cancer cell lines (Varma et al., 2012; Ahmeda et al., 2020). Previous reports revealed that the anticancer activity increases with a decrease in particle size based on their better penetration ability over the cell lines. It has been surveyed that particle size lower than 50 nm displays better activity in the corresponding cancer cell lines (Raut et al., 2010; Varma et al., 2012; Ahmeda et al., 2020). As shown in Figures FE-SEM and HR-TEM of our study, the average size of recent nanocomposite is lower than 50 nm.

3.3. Antioxidant potentials of $AgNO_3$ and Pectin/Ag NPs

Free radicals are highly active compounds with single or unpaired electrons. These compounds are made by metabolic functions in the body during the reaction of oxygen with certain molecules. Free radicals tend to gain or lose an electron so that the number of electrons is even. Free radical damage occurs when radicals collide with other molecules to find electron. Free radicals often take an electron from a nearby molecule and convert it into a new free radical, and then the new free radical repeats the reaction chain sequentially, causing cell damage and DNA damage. DNA damage can lead to a variety of effects, including premature aging and cancer. Free radicals in the body due to the body's natural response to pathogens, metabolism especially lipid oxidation, stress, air pollutants, high-energy electromagnetic waves such as X-rays, foods such as hydrogenated vegetable oils and some drugs such as Adriamycin it is produced (Ahmeda et al., 2020; Al-Muhanna et al., 2015; Hileuskaya et al., 2020; Pallavicini et al., 2017; Zangeneh et al., 2019).
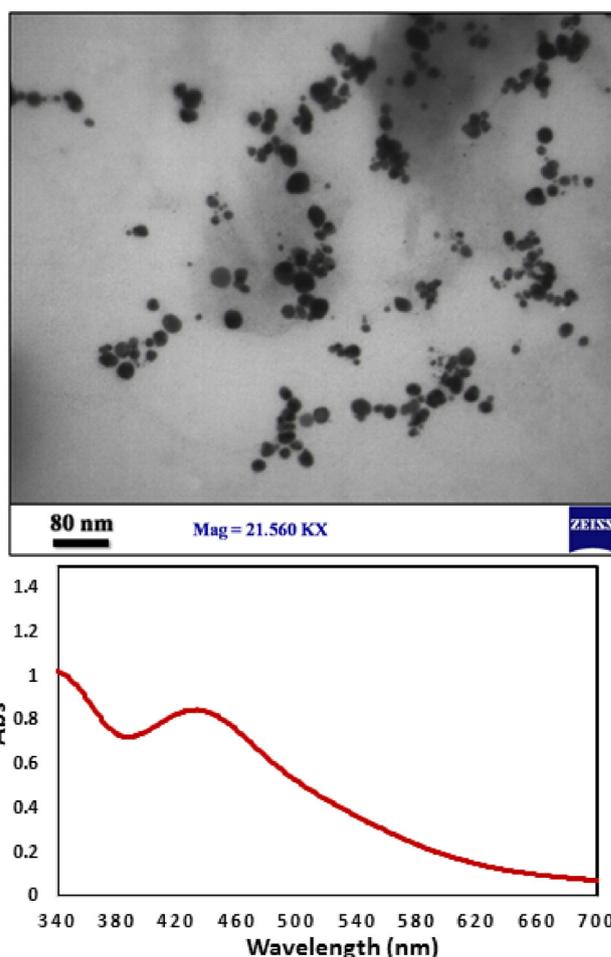
Fig. 8 TEM image and UV–visible spectra of Pectin/Ag NPs after 60 days.

In order to fight the free radicals produced, the cells in the body have intracellular defense due to the presence of the enzymes superoxide dismutase, catalase and glutamine peroxidase. In addition, compounds such as vitamins and minerals (selenium and zinc) with their antioxidant behavior cause the elimination of free radicals and thus reduce their harmful effects on the body. Antioxidants inhibit the free radicals activity or cause them to be removed, and protect the cells of body
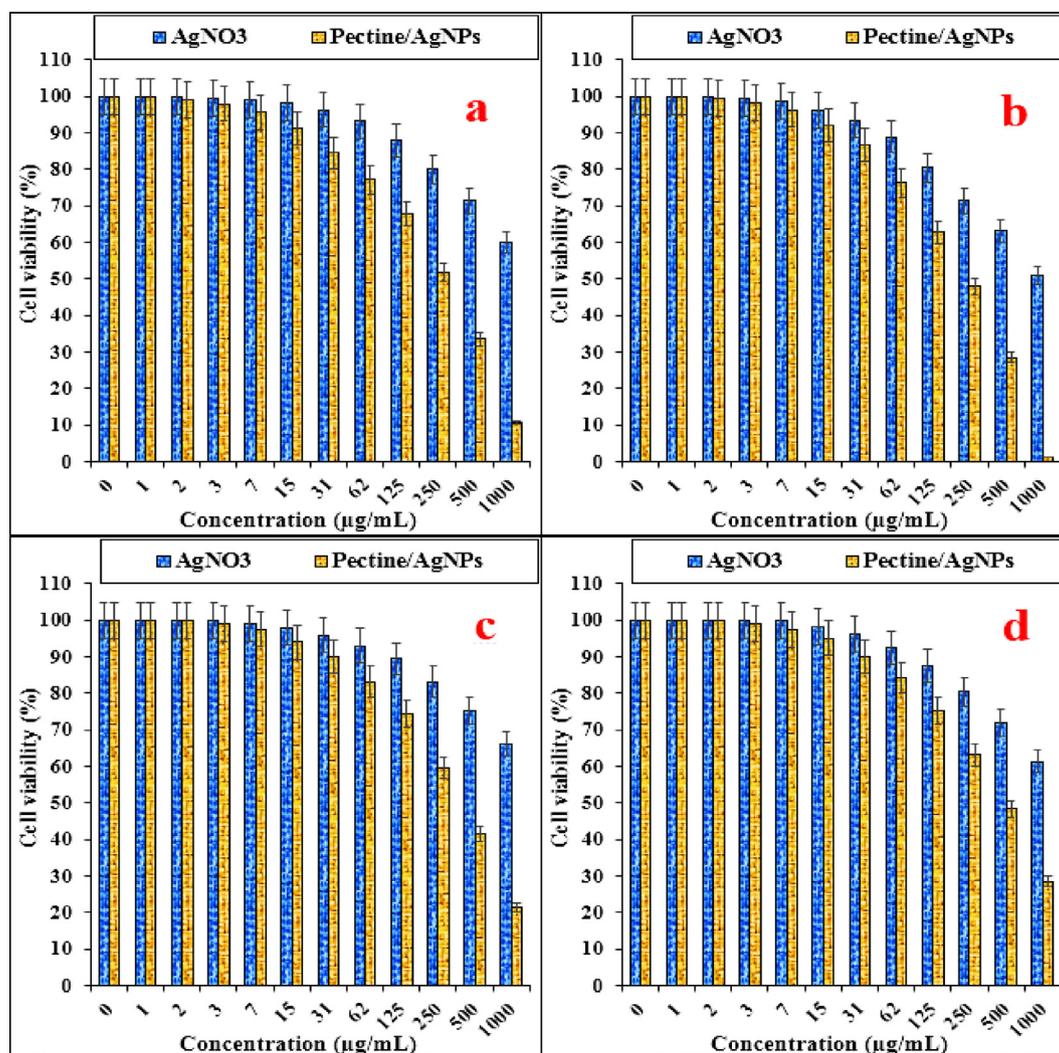
Fig. 9 The anti-colorectal carcinoma properties of AgNO₃ and Pectin/Ag NPs against HT-29 (a), HCT 116 (b), HCT-8 [HRT-18] (c), and Ramos.2G6.4C10 (d) cell lines.

from the wrecking effects of the free radicals. Hence, they fight the aging process and various diseases. These substances can inhibit the formation of free radicals in the body and, if formed, reduce their impact on the body. In fact, antioxidants are compounds that are used to prevent or slow down the damage caused by oxidative reactions in the body and they act as neutralizers of free radicals and therefore prevent damage from these compounds in the body (Aman et al., 2018; Zhaleh and Zangeneh, 2019; Zangeneh et al., 2019). These compounds, on the one hand, reduce the risk of cardiovascular disease and stroke in the first place, and on the other hand, prevent the progression of cancers that cause DNA damage. Despite the presence of various antioxidants in plasma, the body's immune system alone is not able to eliminate free radicals created in the body, therefore, it needs to provide antioxidants from external sources that are provided through food sources. Therefore, the need for strong antioxidants with lower toxicity and greater effectiveness is an inevitable necessity. Antioxidants are also used in industry as food preservatives to prevent spoilage and discoloration of foods, thus increasing the shelf life and shelf life of foods. Plant extracts are one of

the rich compounds of antioxidants (Varma et al., 2012; Ahmeda et al., 2020).

Now, turning our attention to investigate the bioactivity of the AgNO₃ and Pectin/Ag NPs a concentration-dependent DPPH radical scavenging effect of nanomaterial was observed against BHT as a reference. The interaction between the AgNO₃ and Pectin/Ag NPs and DPPH might have occurred by transferring electrons and hydrogen ions (Zangeneh et al., 2019; Aman et al., 2018).

The scavenging capacity of the AgNO₃ and Pectin/Ag NPs and BHT at different concentrations, expressed in terms of percentage inhibition, has been shown in Fig. 11. In the antioxidant test, the IC50 of butylated hydroxytoluene and Pectin/Ag NPs were 181 and 167 µg/mL, respectively (Table 1 and 2).

Metallic nanoparticles green-mediated show higher antioxidant effects against free radicals' formation into the living system (Ahmeda et al., 2020; Zangeneh et al., 2019; Aman et al., 2018). The metallic nanoparticles green-formulated have excellent redox properties and have a significant role in free radicals deactivating (Zangeneh et al., 2019). Previous researches have indicated that flavonoids and phenolic compounds attached to
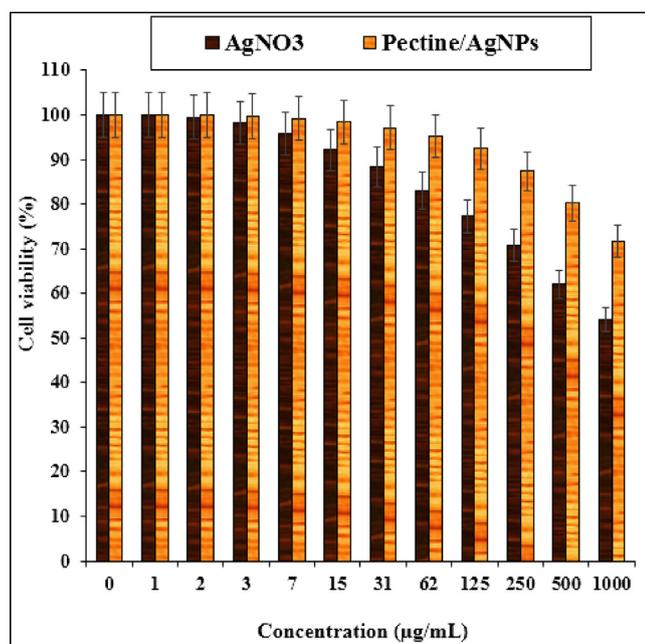
Fig. 10 The cytotoxicity effects of AgNO₃ and Pectin/Ag NPs against Normal (HUVEC) cell line.
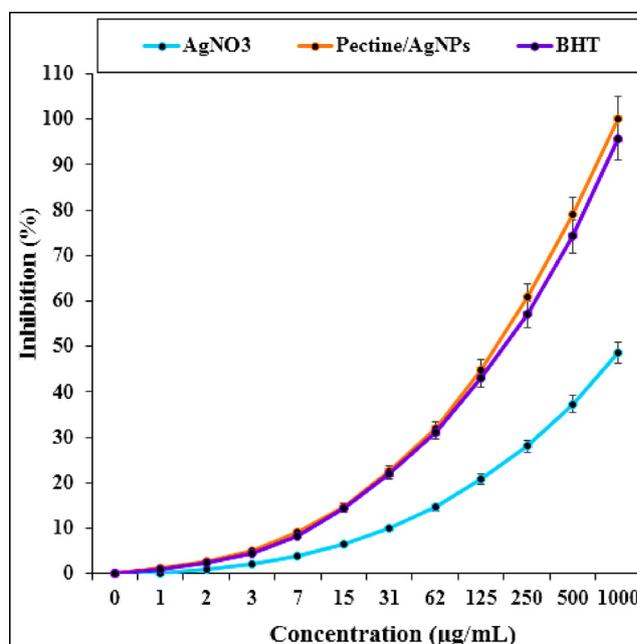
Fig. 11 The antioxidant properties of AgNO₃, Pectin/Ag NPs, and BHT against DPPH.

Table 1 The IC50 of AgNO₃ and Pectin/Ag NPs in the anticolorectal carcinoma test.

	AgNO₃ (μg/mL)	Pectin/Ag NPs (μg/mL)
IC50 against HUVEC	–	–
IC50 against HT-29	–	262 ± 0^a
IC50 against HCT 116	–	236 ± 0^a
IC50 against HCT-8 [HRT-18]	–	393 ± 0^b
IC50 against Ramos.2G6.4C10	–	485 ± 0^c

The various words report significant differences between examined groups ($P \leq 0.01$).

Table 2 The IC50 of AgNO₃, Pectin/Ag NPs, and BHT in the antioxidant test.

	AgNO₃ (μg/mL)	Pectin/Ag NPs (μg/mL)	BHT (μg/mL)
IC50 against DPPH	–	167 ± 0^a	181 ± 0^a

The various words report significant differences between examined groups ($P \leq 0.01$).

the metallic nanoparticles have significant antioxidant properties (Aman et al., 2018).

Oxidation from reactive oxygen species can cause cell membrane disintegration, damage to membrane proteins, and DNA mutation that the result is the onset or exacerbation of many diseases such as cancer, liver damage, and cardiovascular disease. Although the body has a defense system, constant exposure to chemicals and contaminants can lead to an increase in the number of free radicals outside the body's defense capacity and irreversible oxidative damage (Soni and Krishnamurthy, 2013; Katata-Seru et al., 2018; Sangami and Manu, 2017). Therefore, antioxidants with the property of removing free radicals play an important role in the prevention or treatment of oxidation-related diseases or free radicals. Extensive molecular cell research on cancer cells has developed a targeted approach to the biochemical prevention of cancers that the goal is to stop or return cells to their pre-cancerous state without any toxic doses through nutrients and drugs. Numerous studies have been performed on the use of natural compounds as anti-cancer agents in relation to appropriate antioxidant activity (Sangami and Manu, 2017; Beheshtkhoo and Kouhbanani, 2018; Radini et al., 2018). It seems the high anti-human colon carcinoma properties of Pectin/Ag NPs are related to its antioxidant activities. Our successful efforts to utilize Pectin/Ag NPs in carcinoma studies certainly shed light on future studies in this area.

4. Conclusions

In summary we report the green synthesis of Pectin/Ag NPs being synthesized by deposing *in situ* bio-reduced Ag NPs over pectin in an alkaline medium. The material was physico-chemically characterized using UV–Vis and FT-IR spectroscopy, FESEM, EDX, HR-TEM and XRD analysis. The average diameters of the particles were ∼15–20 nm. In the oncological part of the recent study was revealed significant cytotoxicity and anti-human colorectal carcinoma properties of Pectin/Ag NPs against common human colorectal carcinoma cell lines i.e., colorectal adenocarcinoma (HT-29), colorectal carcinoma (HCT 116), ileocecal colorectal adenocarcinoma (HCT-8 [HRT-18]), and Burkitt's lymphoma (Ramos.2G6.4C10) in the *in vitro* condition. The antioxidant properties of Pectin/Ag NPs were determined against DPPH free radicals. The IC50 of Pectin/Ag NPs was 167 µg/mL. Maybe the anti-human colorectal carcinoma properties of Pectin/Ag NPs are related to their antioxidant effects.

Declaration of Competing Interest

The authors declare that they have no known competing financial interests or personal relationships that could have appeared to influence the work reported in this paper.

References

(a) A. Ahmeda, B. Mahdavi, F. Zaker, S. Kaviani, S. Hosseini, M.M. Zangeneh, A. Zangeneh, S. Paydarfar, R. Moradi, Appl Organometal Chem. 34 (2020) e5433. (b) M. Shahriari, S. Hemmati, A. Zangeneh, M.M. Zangeneh. Appl Organometal Chem. 34 (2020) e5476. (c) A. Ahmeda, A. Zangeneh, M.M. Zangeneh. Appl Organometal Chem. 34 (2020) e5290. (d) S. Hemmati, Z. Joshani, A. Zangeneh, M.M. Zangeneh. Appl Organometal Chem. 34 (2020) e5277. (e) S. Hemmati, P. Irani, A. Zangeneh, M.M. Zangeneh. Appl Organometal Chem. 34 (2020) e5274. (f) S. Hemmati, Z. Joshani, A. Zangeneh, M.M. Zangeneh. Appl Organometal Chem. 34 (2020) e5267.

Al-Muhanna, M.K.A., Hileuskaya, K.S., Kulikouskaya, V.I., Kraskouski, A.N., Agabekov, V.E., 2015. Colloid J. 77, 677–684.

S. Aman1, U. K. Gupta, D. Singh, T. Khan1. SGVU J.Pharm. Res. Edu., 3 (2018) 325-329.

Astin, M., Griffin, T., Neal, R.D., Rose, P., Hamilton, W., 2011. Br. J. Gen. Pract. 61, 231–243.

Beheshtkhoo, N., Kouhbanani, M.A.J., Savardashtaki, A., 2018. Appl. Phys. A 124, 363–369.

Cunningham, D., Atkin, W., Lenz, H.J., Lynch, H.T., Minsky, B., Nordlinger, B., Starling, N., 2010. Colorectal cancer. Lancet 375, 1030–1047.

Hileuskaya, K., Ladutska, A., Kulikouskaya, V., Kraskouski, A., Novik, G., Kozerozhets, I., Kozlovskiy, A., Agabekov, V., 2020. Colloids and Surfaces A 585, 124141.

Juul, J.S., Hornung, N., Andersen, B., Laurberg, S., Olesen, F., Vedsted, B., 2018. Br. J. Cancer 119, 471–479.

Katata-Seru, L., Moremedi, T., Aremu, O.S., 2018. J. Mol. Liq. 256, 296–304.

Krishnaraj, C., Jagan, E.G., Rajasekar, S., Selvakumar, P., Kalaichelvan, P.T., Mohan, N., 2010. Colloids Surf. B Biointerf. 76, 50–56.

Lauby-Secretan, B., Scoccianti, C., Loomis, D., Grosse, Y., Bianchini, F., Straif, K., 2016. J. Med. 375, 794–798.

Pallavicini, P., Arciola, C.R., Bertoglio, F., Curtosi, S., Dacarro, G., D'Agostino, A., Ferrari, F., Merli, D., Milanese, C., Rossi, S., Taglietti, A., Tenci, M., Visai, L., 2017. J. Colloid Interface Sci. 498, 271–281.

Radini, I.A., Hasan, N., Malik, M.A., 2018. J. Photochem. Photobiol. B 183, 154–163.

S. Rajeshkumar, C. Kannan, G. Annadurai, Drug Invention Today 4 (2012) 511–513.

a) R. W. Raut, N. S. Kolekar, J. R. Lakkakula, V. D. Mendhulkar, S. B. Kashid, Nano-Micro Lett. 2 (2010) 106-113; b) H. Veisi, S. Hemmati, P. Safarimehr, J. Catal. 365 (2018) 204-212; c) S. Mirfakhraei, M. Hekmati, F.H. Eshbala, H. Veisi, New J. Chem. 42 (2018) 1757-1761; d) M. Baghayeri, A. Amiri, Z. Alizadeh, H. Veisi, E. Hasheminejad, J. Electroanal. Chem. 810 (2018) 69-77.

Sangami, S., Manu, M., 2017. Environ. Technol. Innov. 8, 150–163.

Shaib, W., Mahajan, R., El-Rayes, B., 2013. J. Gastrointest. Oncol. 4, 308–318.

Soni, A., Krishnamurthy, R., 2013. Indian J. Plant. Sci. 2, 117–125.

(a) R. S. Varma, Curr. Opin. Chem. Eng., 1 (2012) 123; (b) M. Entezari, M. Safari, M. Hekmati, S. Hekmat, A. Azin, Med. Chem. Res. 23 (2014) 487-495; (c) M Hajighorbani, M Hekmati, RSC advances, 2016,6, 88916-88924; (d) J. Azizian, M. Hekmati, O.G. Dadras, Orient J Chem 30 (2014) 667-673; (e) M.H. Salehi, M. Yousefi, M. Hekmati, E. Balali, Polyhedron 165 (2019) 132-137; (f) Z. Karimi Ghezeli, M. Hekmati, H. Veisi, Applied Organometallic Chemistry 33 (2019) e4833; (g) R. Ghorbani-Vaghei, S. Hemmati, M. Hekmati, Journal of Chemical Sciences 128 (2016) 1157-1162; (h) Wei Zhang, Hojat Veisi, Reyhaneh Sharifi, Delafarin Salamat, Bikash Karmakar, Malak Hekmati, Saba Hemmati, Mohammad Mahdi Zangeneh, Zhiyong Zhang, Qiang Su, Int J Biological Mac. 160 (2020) 1252-1262; (i) H. Veisi, Y. Metghalchi, M. Hekmati, S. Samadzadeh, Appl. Organomet. Chem. 31 (2017) e3676; (j) H. Veisi, P. Safarimehr, S. Hemmati, Mate. Sci. Eng. C 96 (2019) 310-318; (k) H. Veisi, A. Sedrpoushan, A.R. Faraji, M. Heydari, S. Hemmati, B. Fatahi, RSC Advances 5, 84 (2015), 68523-68530.

Zangeneh, M.M., Bovandi, S., Gharehyakheh, S., Zangeneh, A., Irani, P., 2019a. Appl. Organomet. Chem. 33, e4961.

Zangeneh, M.M., Saneei, S., Zangeneh, A., 2019b. Appl. Organometal. Chem. 33, e5216.

Zhaleh, M., Zangeneh, A., Goorani, S., 2019. Appl. Organometal. Chem. 33, e5015.